$\underline{R}_{b0} = \underline{R}_{a0} = \underline{X}_b = \underline{X}_a = 3.0$

$\underline{RX}_b = \underline{RX}_a = 1.0$

$k_1 = k_2 = k_3 = k_4 = k_5 = k_6 = k_7 = k_8 = 1.0$

$\underline{AB}(t)$ = ratio of molecules formed by the reaction of transmitter A and transmitter B to T.

$(\underline{AB})_N(t)$ = ratio of molecular conglomerates of N (AB) molecules to T.

$(\underline{AB})_N \underline{R}_b(t)$ = ratio of receptor sites for transmitter B combined with $(AB)_N$ to T. Sites blocked with $(AB)_N$ are unable to react with transmitter B and hence do not assist in bringing about the conductance change which leads to the depolarization of control neuron C_2.

k_9, controls combination rate of transmitter A and transmitter B, $= 10.0$

k_{10}, controls the rate for the combination of N AB molecules into complex $(AB)_N$, $= 1.0$

k_{11}, controls the decay of AB due to enzyme hydrolysis and/or diffusion, $= 0.005$

k_{12}, controls the decay of $(AB)_N$ due to enzyme hydrolysis and/or diffusion, $= 0.0002$

k_{13}, controls combination rate of $(AB)_N$ and receptor sites for transmitter B, $= 1.0$

k_{14}, long term decay constant of $(AB)_N R_b$ or equivalent, $= 0.0$.

References

Arbib, M. A.: Brains, machines and mathematics. New York: McGraw-Hill 1964.

Curtis, D. R., Eccles, R. M.: The effect of diffusional barriers upon the pharmacology of cells within the central nervous system. J. Physiol. (Lond.) **141**, 446—463 (1958).

Eccles, J. C.: The physiology of synapses. Berlin-Göttingen-Heidelberg: Springer 1964.

— Jaeger, J. C.: The relationship between the mode of operation and the dimensions of the junctional regions at synapses and motor end-organs. Proc. roy. Soc. B **148**, 38—56 (1958).

Galambos, R.: A glial-neural theory of brain function. Proc. nat. Acad. Sci. (Wash.) **47**, 129—136 (1961).

Good, I. J.: Discussion following paper by Farley and Clark. Information Theory, ed. C. Cherry, p. 249. Washington: Butterworth 1961.

Griffith, J. S.: A theory of the nature of memory. Nature (Lond.) **211**, 1160—1163 (1966).

— A view of the brain. Abingdon: Oxford Univ. Press 1967.

Hebb, D. O.: The organization of behavior: a neurophysiological theory. New York: Wiley 1949.

Horridge, G. A.: Interneurons. London: Freeman 1968.

Hydén, H., Egyházi, E.: Glial RNA changes during learning experiments in rats. Proc. nat. Acad. Sci. (Wash.) **49**, 618—624 (1963).

John, E. R.: Mechanisms of memory. New York: Academic Press 1967.

Kandel, E. R., Tauc, L.: Heterosynaptic facilitation in neurons of the abdominal ganglion of *Aplysia depilans*. J. Physiol. (Lond.) **181**, 1—27 (1965).

Katz, B.: Nerve, muscle, and synapse. New York: McGraw-Hill 1966.

Kennedy, D., Evoy, W. H., Hanawalt, J. T.: Release of coordinated behavior in crayfish by single central neurons. Science **154**, 917—919 (1966).

Kimble, G. A.: Hilgard and Marquis, Conditioning and learning, revised. New York: Appleton-Century-Crofts 1961.

Krnjević, K., Mitchell, J. F.: The release of acetylcholine in the isolated rat diaphragm. J. Physiol. (Lond.) **155**, 246—262 (1961).

Milner, P. M.: Learning in neural systems. In: Self-organizing systems, eds. Yovits, M., Cameron, S., p. 190—202. Oxford: Pergamon Press 1960.

Payton, B. W., Bennett, M. V. L., Pappas, G. D.: Temperature-dependence of resistance at an electrotonic synapse. Science **165**, 594—597 (1969).

Pfaff, D.: Parsimonious biological models of memory and reinforcement. Psychol. Rev. **76**, No. 1, 70—81 (1969).

Rosenblatt, F.: Principles of neurodynamics. Washington: Spartan Books 1962.

— Recent work on theoretical models of biological memory. In: Computer and information sciences II., ed. Tou, J. T., p. 33—56. New York: Academic Press 1967.

Siekevitz, P., Palade, G., Dallner, G., Ohad, I., Omura, T.: The biogenesis of intracellular membranes. In: Organizational biosynthesis, eds. Vogel, H., Lampen, J., Bryson, V., p. 331—362. New York: Academic Press 1967.

Stevens, C. F.: Synaptic physiology. Proc. of the IEEE, Special Issue on Studies of Neural Elements and Systems **56**, No. 6, 916—930 (June 1968).

Vladimirova, I. A., Kosareva, V. Z., Storozhuk, V. M.: Estimated number of active neurons in the primary somatosensory cortex of cats. Neurosci. Trans. No 6, 727—733 (1969).

Walker, E. L.: Conditioning and instrumental learning. Belmont: Brooks/Cole 1967.

Waser, P. G.: The cholinergic receptor. J. Pharm. Pharmacol. **12**, 577—594 (1960).

J. R. Birk
Bioengineering Laboratory
The University of Connecticut
Storrs, Conn., 06268, USA

Linearizing: A Method for Analysing and Synthesizing Nonlinear Systems

Henk Spekreijse and Hans Oosting
Laboratory of Medical Physics, University of Amsterdam, Amsterdam

Received November 28, 1969

Summary. Physical and especially biological systems behave many times in such a way that the methods of linear system analysis are not adequate, even when "small" signals are used.

This paper presents an approach which has been applied succesfully in the analysis of certain nonlinear biological systems. The method is capable to recognize in these systems the linear and nonlinear elements. Furthermore these elements can be characterized and a functional sequence can be detected. Applications of the method are illustrated for the analysis of two biological systems and the synthesis of a physical system.

Introduction

Linear input-output relationships may be a valid idealisation for physical systems, but biological systems exhibit more frequently a nonlinear behavior. Nevertheless it is common to use techniques of linear system analysis for the study of these systems, since linear techniques have general applicability and are quite straight forward. In contrast, the analysis of a nonlinear system is much more complicated and any nonlinear system may present a fresh problem to be solved on its own terms with a "custom designed" approach. In some cases, however, more information about the system, such as the organization of successive stages, can be extracted from a nonlinear than from a linear system.

In this paper a method will be introduced that can determine the *sequence* of linear and nonlinear transformations in certain nonlinear systems. This possibility contrasts with the case of linear systems where

the sequence of transformations can never be determined from the response of the system as a whole. We shall outline our method in part I of this paper, but we must emphasize that this is not a general approach. Part II covers the mathematical treatment and part III describes applications of the method. The first two applications deal with the analysis of two biological systems, namely ganglion cell responses in the goldfish retina, and scalp potentials evoked in man by spatially unstructured visual stimuli. The third application is the synthesis of a physical system — in this case a polarity coincidence correlator.

I. Outline of the Method

I.1. Linear versus Nonlinear

A system is defined as linear if the superposition principle holds for it. Fourier's theorem states that any periodic signal can be written as a sum of sinusoids, each with its own amplitude and phase. Therefore the response of a linear system to *any* type of periodic input signal can be calculated when the behavior of the system is known as a function of the frequency of a sinusoid input signal. This allows the dynamic properties of a linear system to be fully described by two characteristics only; namely the amplitude characteristic and the phase characteristic. In contrast with many nonlinear systems both characteristics, and therefore also the dynamic behavior of a linear system, are *independent* of the amplitude of the input signal.

All systems for which the superposition principle does not hold are nonlinear. In addition a sinusoidal input to such a system can give rise to an output signal that may contain frequencies other than the input frequency. In this paper we restrict ourselves to a special class of nonlinearities: the zero-memory single valued nonlinearities. The response of these nonlinearities depends only on the amplitude and not on the frequency of a (sinusoidal) input signal. A commonly used graphic representation of such a purely amplitude distorting element is given in Fig. 1. This figure shows the distortion produced by a "leaky" diode with characteristic $y=f(x)$ to a sinusoidal input $x(t)=A\sin\omega t$. Because the input signal is periodic and the nonlinearity is of a single valued type Fourier's theorem can be used to make a *harmonic* analysis of this output signal. In general each harmonic component in the series will have an amplitude and phase which depends on the amplitude of the sine wave input signal. This allows zero-memory single valued nonlinearities to be classified as follows:

a) Smooth Static Nonlinearities. These are systems for which the function $f(x)$ and all its derivatives are bounded continuous functions of x in the range of input amplitudes A ($|x|\leqq A$). A power series expansion of $f(x)$ is always possible for these systems. This means that if the amplitude of a (sinusoidal) input is decreased, the result is that the amplitudes of the harmonics in the response are reduced in such a way that the attenuation is greater the higher the order of the harmonic. In other words, the output waveform grows more and more like the input sinusoid as the amplitude of the input is progressively reduced. These systems can therefore be investigated under such conditions that their behavior is approximately linear, i.e. by using "small" signals.

b) Essential Static Nonlinearities. These are systems for which $f(x)$ or one of its derivatives are discontinuous for one or more values of x, such that $|x|\leqq A$. If the average value of the input signal takes a value of x_0, and $f(x)$ or one of its derivatives is discontinuous at $x=x_0$, then the Fourier expansion of the output signal of the nonlinearity to a sinusoidal input includes harmonics whose amplitude spectrum is independent of the amplitude of the input signal. In practice this means that if the input amplitude is progressively decreased then there is *no reduction* of the harmonic content in the output of this type of nonlinearity.

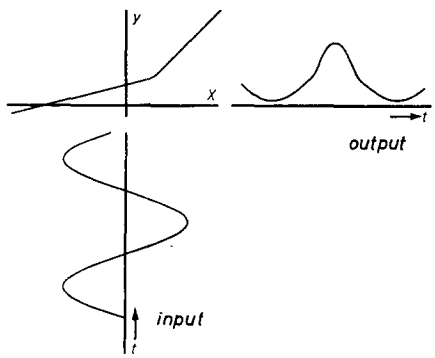

Fig. 1. A commonly used graphic representation of the response of a purely amplitude distorting element, in this case a diode, to a sinusoidal input signal

I.2. Linearizing

Since the problem of analysing the second type of nonlinearity is not reduced by using "small" signal conditions it was necessary to develop another method. It turns out that the harmonic content found in the response of an essential static nonlinearity to a sinusoidal stimulus can be changed by adding an auxiliary input to the input sine wave*. The effect on the response of adding an auxiliary Gaussian noise to the sinusoidal signal is illustrated for an ideal half-wave rectifier: ($y=x$ for $x\geqq 0$; $y=0$ for $x<0$) in the left column of Fig. 2. The Fourier series representation of the output signal of this rectifier to an input sinusoid $x(t)=A\sin\omega t$ solely (see Fig. 2a) is:

$$y(t)=\frac{A}{\pi}+\frac{A}{2}\sin\omega t - \frac{2A}{\pi}\left\{\frac{1}{1.3}\cos 2\omega t+\frac{1}{3.5}\cos 4\omega t+\frac{1}{5.7}\cos 6\omega t+\cdots\right\}.$$

As is evident from this expression, the ratio of the amplitudes of the output harmonics is independent of the amplitude of the input sine wave. An auxiliary noise added to the sinusoidal input signal acts as a "carrier" whose effect is to shift the amplitude domain of the signal sine wave away from the breakpoint in the rectifier. On the average the sine wave signal is then more often in a region where $f(x)$ is linear (Fig. 2b). Therefore the breakpoint is masked more and more as the signal to noise ratio is reduced, and

* "The auxiliary input" must be uncorrelated with the sine wave signal and may take quite a number of forms: Gaussian noise, sinusoid, triangle etc.

the system gives a progressively more sinusoidal response*. If the dc-component in the response is neglected, then the averaged response approximates to:

$$y(t) = \frac{A}{2} \sin \omega t.$$

A minor point is that the output of the fundamental component is only half the input amplitude; this originates from the fact that the auxiliary noise produces a shift which in this case is symmetrical about zero.

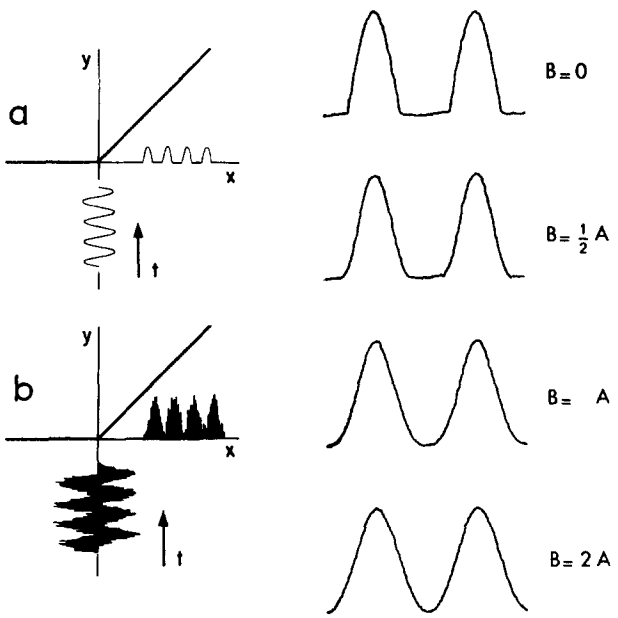

Fig. 2. Left column shows diagrammatically the response of a linear half-wave rectifier for a sine wave input signal (a) and for a sine wave with added noise (b). Right column figures show the linearizing effect of a sine wave auxiliary signal ($B \sin \beta t$) added to a sine wave stimulus ($A \sin \omega t$). These output signals of a half-wave linear rectifier are averaged with a CAT computer, whose sweep is triggered by the sine wave stimulus ($A \sin \omega t$) ($\omega = 8$ cps; $\beta = 11$ cps). The upper figure shows the familiar half-wave rectified sine wave, obtained without adding an auxiliary signal, i.e. $B = 0$. With increasing amplitude B the distortion in the response reduces, until for $B = 2A$ an almost pure sinusoid is obtained (bottom figure). Comparison of upper and bottom figure shows that the amplitude of the fundamental component in the response is not effected by the auxiliary signal. This is characteristic for a half-wave linear rectifier

It can be shown that the output of a static nonlinearity is linearized not only by Gaussian noise but also by almost any periodic auxiliary signal, such as sinusoids, square waves, triangles, etc. The right column of Fig. 2 gives an example of how the output of a half-wave linear rectifier can be linearized by increasing the amplitude B of an added auxiliary sinusoid.

The effect of the various auxiliary signals upon the amplitudes of the output harmonics can be calculated for different types of nonlinearities (see II). As could be expected the relation between the amplitudes of the output harmonics and the signal to "noise" ratio depends on the characteristic of the nonlinearity. For example, changing the amplitude of the input "noise" — in this case an auxiliary sinusoid — does not affect the amplitude of the fundamental component ($n = 1$) in the response of a linear rectifier, while in contrast, the amplitude of this component does alter in a quadratic rectifier. For the latter, however, the amplitude of the second harmonic ($n = 2$) remains constant (Fig. 3).

It follows from this that the relationship between on the one hand the relative amplitudes of the output harmonics, and on the other hand the input signal to

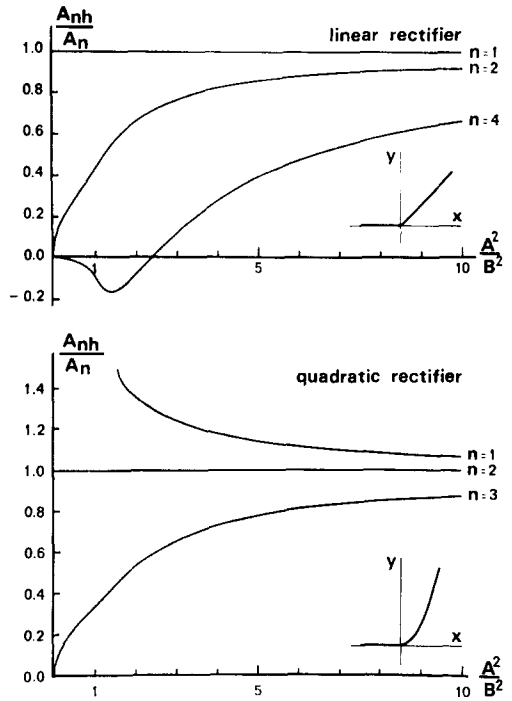

Fig. 3. Linearizing effect of a sinusoidal auxiliary signal ($B \sin \beta t$) added to a sinusoidal stimulus ($A \sin \omega t$) for a half-wave linear and a half-wave quadratic rectifier. The figures show, as a function of the signal to "noise" ratio A^2/B^2, the calculated amplitude ratios A_{nh}/A_n for different values of n. A_n is the amplitude of the n-th harmonic in the output signal for a sinusoidal input; and A_{nh} is the (averaged) amplitude of the n-th harmonic in the output for a sinusoidal input plus an auxiliary signal. These curves show that the variation in the amplitudes of the harmonics with the input signal to "noise" ratio enables the determination of the characteristic of the rectifier

"noise" ratio, can be used to determine the characteristics of the nonlinearity. There is of course no need to use such an elaborate method for merely measuring the characteristics of a static nonlinearity. The power of our method, as we shall show below, lies in its ability to determine the functional sequence of linear and nonlinear transformations in a system which contains a static nonlinearity. In addition, the linearizing phenomena can be used to determine the characteristics of the various individual elements.

I.3. Lumped Nonlinear Systems

The simple lumped nonlinear system shown in Fig. 4 will be used to demonstrate the linearizing method. This system consists of two linear elements [with transfer functions $H_1(j\omega)$ and $H_2(j\omega)$ respectively] which are separated by a single-valued zero-memory nonlinearity $z = f(y)$. Given a sinusoidal signal

* It is not the "raw" response which is linearized but the response after time-locked averaging; see II.

$x(t)$, then the output signal $y(t)$ of the first linear element $H_1(j\omega)$ is also a sinusoid. The relations between the amplitudes and phases of the input and output sinusoids are determined only by the *frequency* of the input sinusoids. On the other hand, the output of the type of nonlinear element chosen depends only on the *amplitude* of the input sine wave $y(t)$. Therefore the input sinusoid contains two parameters, for one of which (amplitude) the nonlinearity is sensitive and for the other of which (frequency) the linear element is sensitive. Since these two parameters can be varied independently of each other, it is in principle possible to determine the individual characteristics of the linear and the nonlinear elements.

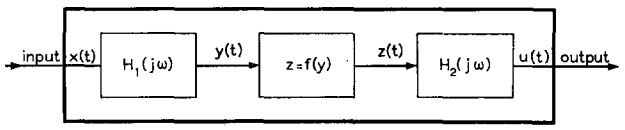

Fig. 4. A nonlinear system consisting of two linear elements with transfer functions $H_1(j\omega)$ and $H_2(j\omega)$ respectively, which are separated by a single-valued zero-memory nonlinearity $z=f(y)$

As previously mentioned, when the input signal $x(t)$ is sinusoidal, then the input to the nonlinearity is also a sinusoid. However, knowledge of the input waveform to the nonlinear element is not sufficient to determine the characteristic $z=f(y)$, since the amplitudes of the output harmonics are still weighted by the second linear element $H_2(j\omega)$. When an auxiliary sine wave $B\sin\beta t$ is added to the sinusoidal input signal, then the incoming signal to the nonlinearity consists of the algebraic sum of the separate responses of the first linear element to the sinusoidal stimulus and the supplementary signal. In general two frequencies ω and β can be selected such that, when they reach the nonlinearity, the ratio of the amplitudes of these two sine waves is approximately the same as at the input of the whole system. By varying the signal to "noise" ratio, the amplitudes of the output harmonics of the system can be measured as a function of the signal to "noise" ratio at the input of the nonlinear element. A graph similar to that shown in Fig. 3 results. The shape of the curves in this graph depends only on the characteristic of the nonlinearity and not at all on the transfer functions $H_1(j\omega)$ and $H_2(j\omega)$. The characteristic $f(y)$ of the nonlinearity can be calculated from this graph. If, however, the curves prove to be complicated functions, it is preferable to determine first the amplitude and phase characteristics of the linear element $H_1(j\omega)$.

The Amplitude Characteristic $H_1(\omega)$ can be determined from the way in which the linearizing effect of the sinusoidal auxiliary signal upon one of the output harmonics varies as a function of its frequency β. The sinusoidal input signal must retain the same frequency in the successive experiments, so as to keep the influence of the transfer function $H_2(j\omega)$ constant. Suppose that in the linearizing experiment described above, measurements of the second harmonic had been used to determine the amplitude characteristic of the first linear element $H_1(j\omega)$ and suppose also for simplicity that the signal to "noise" ratio (A/B) at the input of $H_1(j\omega)$ was kept constant. Assume next that doubling the frequency of the auxiliary signal increased the ratio A_{2h}/A_2 from 0.4 to 0.7. By comparing these data with the linearizing graph it would have been found that for example, $A_{2h}/A_2=0.4$ for $(A/B)^2=1$ and $A_{2h}/A_2=0.7$ for $(A/B)^2=4$ at the input of the nonlinearity. Thus, in this hypothetical case, the amplitude of the auxiliary sinusoid would have been reduced by a factor of 2 as its frequency was raised by one octave. This would mean that the first linear element $H_1(j\omega)$ had an attenuation of 6 db/octave in the frequency range $\beta-2\beta$. By repeating the procedure for various frequencies β the entire amplitude characteristic of $H_1(j\omega)$ could be obtained.

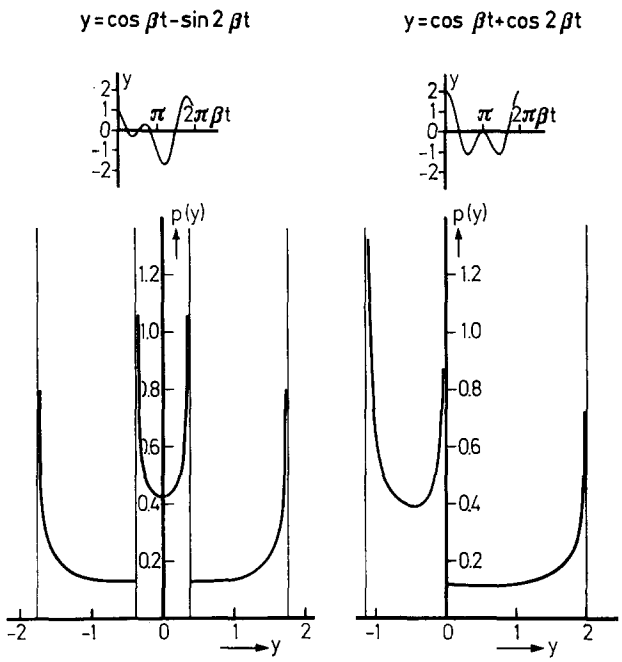

Fig. 5. Amplitude density distribution of a waveform that consists of two cosines with equal amplitudes and periodicities β and 2β. As shown, this distribution is a function of the relative phase ϕ between the two cosines. Hence, also the linearizing effect of this waveform depends on the relative phase

Phase Characteristic, $\phi_1(\omega)$. Only for a linear minimum-phase shift system are the amplitude and phase characteristics in a one to one relation with each other. Since considerable phase shifts due to delay are not uncommon, especially in biological systems, it may be useful to determine the phase characteristic $\phi_1(\omega)$ of the first linear element. This phase characteristic can be determined by using an auxiliary signal which consists of two sine waves with frequencies β and 2β. Since the amplitude characteristic of $H_1(j\omega)$ is available by using the method described above the amplitudes of the two sine waves, with frequencies β and 2β, can be chosen in such a way that they are equal at the input of the nonlinearity.

As will be shown in II the linearizing effect of an auxiliary signal is a function of its amplitude density distribution. Fig. 5 shows that the amplitude density distribution $p(y)$ of the auxiliary signal $y(t)=\sin\beta t+\sin(2\beta t+\phi)$ is a function of the phase ϕ between the two constituent sinusoids. This means that

the linearizing effect of the waveform $y(t)$ is also a function of the relative phase ϕ between the two sinusoids at the input of the static nonlinearity. The phase is known at the input of $H_1(j\omega)$ and thus the phase shift due to this process is also known over one octave. By repeating the procedure for various frequencies β, the phase characteristic of the $H_1(j\omega)$ can be determined from the way in which the amplitude of a single harmonic in the output of the entire system varies as a function of the frequencies in the auxiliary signal. This is illustrated in Fig. 6 for a half-wave linear rectifier. The graph illustrates (see also Fig. 3) that two sinusoidal auxiliary inputs may have a smaller

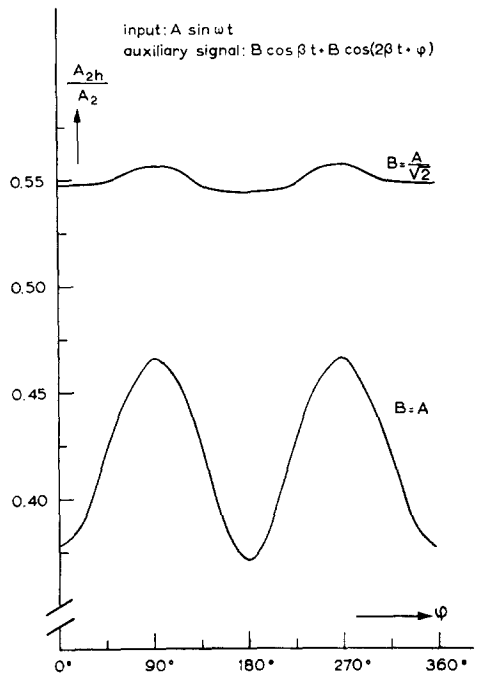

Fig. 6. Linearizing effect of an auxiliary signal, which is the sum of two sinusoids, upon the second harmonic in the output of a linear half-wave rectifier to a sinusoidal input $A \sin \omega t$. The figure shows the amplitude ratio of the second harmonic A_{2h}/A_2 as a function of the relative phase ϕ. The dependence of this ratio on the relative phase ϕ becomes stronger for decreasing signal to "noise" ratio, since the slope of the linearizing curve increases for decreasing values of N (see Fig. 3)

linearizing effect than one sinusoidal auxiliary input only. This may occur even when the two sinusoidal auxiliaries have a larger peak to peak amplitude than a single auxiliary sinusoid.

The Transfer Characteristic $H_2(j\omega)$ can now be determined by direct sinusoidal measurement, i.e. without an auxiliary signal, since we know the characteristics of the first frequency dependent element. This allows us to keep the input sine wave to the nonlinearity constant in amplitude and phase. Since the nonlinearity is static, its output harmonics are then also constant in amplitude and phase, independently of the frequency of the sinusoidal input signal. Therefore the input signal to $H_2(j\omega)$ is known, and hence the transfer function of the second linearity can be determined by varying the frequency of the input sinusoid $x(t)$ to the entire system.

A more elegant method, however, is to obtain the crosscorrelogram between the input signal and the response of the whole system. With white noise as the input signal it can be shown that this crosscorrelogram represents the impulse response of the linear elements in the system only (Bussgang, 1952). However, it should be noted that the sequence of the processes can not be found by this method (see also II.3).

II. Mathematical Treatment

The mathematical treatment is restricted to the class of nonlinearities for which the Laplace transform exists. It has been found that many physical and biological systems can be described in terms of this type of nonlinearity.

II.1. General Computation of A_n and A_{nh}

Let in the domain $\alpha < \mathrm{Re}\,\xi < \beta$ the function $F(\xi)$ be the two-sided Laplace transform of a single valued zero-memory nonlinearity $y = f(x)$. Then:

$$y = f(x) = \frac{1}{2\pi j} \int_{c-j\infty}^{c+j\infty} F(\xi) \exp(\xi x)\, d\xi, \qquad (1)$$

with $\alpha < c < \beta$.

For an input signal $x(t) = A \cos \omega t + h(t)$, where $h(t)$ is the auxiliary signal, Eq. (1) becomes:

$$y(t) = \frac{1}{2\pi j} \int_{c-j\infty}^{c+j\infty} F(\xi) \exp[\xi A \cos \omega t] \cdot \exp[\xi h(t)]\, d\xi. \qquad (2)$$

By use of the Jacobi-Anger formula:

$$\exp[\xi A \cos \omega t] = \sum_{n=0}^{\infty} \varepsilon_n I_n(A\xi) \cos n\omega t; \qquad (3)$$

where ε_n is the Neumann factor $\varepsilon_0 = 1$, $\varepsilon_n = 2$ $(n = 1, 2, \ldots)$ and I_n is the modified Bessel function of the first kind. Hence it follows that:

$$y(t) = \frac{1}{2\pi j} \sum_{n=0}^{\infty} \varepsilon_n \cdot \left[\int_{c-j\infty}^{c+j\infty} F(\xi) I_n(A\xi) \exp[\xi h(t)]\, d\xi \right] \cos n\omega t. \qquad (4)$$

The auxiliary signal $h(t)$ is added in order to linearize the harmonics in $y(t)$ which originate from the sinusoidal input signal. The contribution of $h(t)$ to the output signal can be reduced by time-locked averaging of $y(t)$. This operation can mathematically be expressed as the crosscorrelation of the signal $y(t)$ with a periodic δ-function with periodicity ω_0 and whose area amounts to T_0 per period $(T_0 = 2\pi/\omega_0)$:

$$\phi_{12}(\tau) = \lim_{T\to\infty} \frac{1}{T} \int_0^T y(t) \sum_{m=0}^{K} \delta(t - m T_0 - \tau)\, dt \qquad (5)$$

where $T = K T_0$.

Substitution of Eq. (4) in the above expression gives:

$$\phi_{12}(\tau) = \lim_{T\to\infty} \frac{1}{T} \int_0^T \sum_{m=0}^{K} \sum_{n=0}^{\infty} \int_{c-j\infty}^{c+j\infty} F(\xi) I_n(A\xi) \cdot \exp[\xi h(t)]\, d\xi \cos n\omega_0 t \times \delta(t - m T_0 - \tau)\, dt. \qquad (6)$$

If $h(t)$ is an ergodic signal with a first order amplitude density distribution $p(h)$, its moment generating function $M_h(\xi)$ is:

$$M_h(\xi) \equiv \int_{-\infty}^{+\infty} \exp(\xi h)\, p(h)\, dh .$$

Since $h(t)$ is ergodic, $M_h(\xi)$ can also be expressed as a time average:

$$M_h(\xi) = \lim_{T\to\infty} \frac{1}{T} \int_0^T \exp[\xi h(t)]\, dt .$$

By a simple limiting operation, the last expression can be shown to be equal to:

$$M_h(\xi) = \lim_{K\to\infty} \frac{1}{K} \sum_{m=0}^{K} \exp[\xi h(m T_0)] .$$

Substitution of the above expression in Eq. (6) gives:

$$\phi_{12}(\tau) = \sum_{n=0}^{\infty} \frac{\varepsilon_n}{2\pi j} \int_{c-j\infty}^{c+j\infty} F(\xi)\, I_n(A\xi)\, M_h(\xi)\, d\xi \cos n\omega_0 \tau . \quad (7)$$

Thus the amplitude A_{nh} of the n-th harmonic originating from the sinusoidal input signal plus ergodic auxiliary signal is:

$$A_{nh} = \frac{\varepsilon_n}{2\pi j} \int_{c-j\infty}^{c+j\infty} F(\xi)\, I_n(A\xi)\, M_h(\xi)\, d\xi ; \quad n = 0, 1, 2, \ldots . \quad (8)$$

When $h(t) = 0$; $M_h(\xi) = 1$. The amplitudes of the harmonics in the output of a purely sinusoidally driven nonlinearity $f(x)$ are then:

$$A_n = \frac{\varepsilon_n}{2\pi j} \int_{c-j\infty}^{c+j\infty} F(\xi)\, I_n(A\xi)\, d\xi ; \quad n = 0, 1, 2, \ldots . \quad (9)$$

II.2. Calculation of A_{nh} and A_n for a Few Nonlinearities

We shall restrict ourselves to a particular class of nonlinearities which are discontinuous only at $x = 0$. It is not a fundamental limitation to consider only the half-wave types of this class of nonlinearities:

$$y = \sum_{\nu=0}^{\infty} a_\nu x^\nu, \qquad x \geqq 0$$
$$y = 0, \qquad x < 0 .$$

Since the Laplace transform is linear, one has under certain restrictions (Papoulis, 1962):

$$L\left\{\sum_{\nu=0}^{\infty} a_\nu x^\nu\right\} = \sum_{\nu=0}^{\infty} L\{a_\nu x^\nu\},$$

and the influence of an auxiliary signal upon the system response can be examined for each individual term in the power series expansion. Therefore it is sufficient to consider the restricted system:

$$y = a_\nu x^\nu, \qquad x \geqq 0$$
$$y = 0, \qquad x < 0 .$$

Laplace transformation of the above characteristic gives:

$$F(\xi) = a_\nu \Gamma(\nu+1)/\xi^{\nu+1} . \quad (10)$$

Substitution in Eq. (9) gives:

$$A_n = \varepsilon_n a_\nu \frac{A^\nu}{2^{\nu+1}} \cdot \frac{\Gamma(\nu+1)}{\Gamma\left(1+\frac{n+\nu}{2}\right)\Gamma\left(1-\frac{n-\nu}{2}\right)} . \quad (11)$$

The frequency β of the sinusoidal auxiliary signal $h(t) = B \sin\beta t$ must be chosen such that for the range of values of n and k of practical interest $n\omega \neq k\beta$ ($n = 1, 2, 3, \ldots$ and $k = 1, 2, 3, \ldots$). Then the output harmonics of the nonlinearity that arise from the auxiliary signal are of different frequencies to the output harmonics evoked by the sinusoidal stimulus. The amplitude density distribution of $h(t)$ is:

$$p(h) = \frac{1}{\pi\sqrt{B^2 - h^2}}, \qquad [h(t)] \leqq B$$
$$p(h) = 0, \qquad [h(t)] > B .$$

Taking the moment generating function $M_h(\xi)$ of $p(h)$ and substitution of $M_h(\xi)$ in Eq. (8) gives:

$$A_{nh} = \frac{\varepsilon_n a_\nu \Gamma(\nu+1)}{2\pi j} \int_{c-j\infty}^{c+j\infty} \frac{I_n(A\xi)\, I_0(B\xi)}{\xi^{\nu+1}}\, d\xi . \quad (12)$$

Eq. (12) is the Weber-Schafheitlin integral. Calculation (see Watson, 1962) gives:

for $A > B$

$$A_{nh} = \frac{\varepsilon_n a_\nu \Gamma(\nu+1)\sin(n-\nu)\frac{\pi}{2} \cdot A^\nu \left(\frac{n-\nu}{2}\right)}{\pi \cdot 2^{\nu+1}\Gamma\left(1+\frac{n+\nu}{2}\right)} \cdot {}_2F_1\left(\frac{n-\nu}{2}, -\frac{n+\nu}{2}; 1; \frac{1}{N_s}\right)^* \quad (13)$$

and for $A < B$

$$A_{nh} = \frac{\varepsilon_n a_\nu \Gamma(\nu+1)\sin(n-\nu)\frac{\pi}{2} \cdot N_s^{n/2} B^\nu \Gamma\left(\frac{n-\nu}{2}\right)}{\pi \cdot 2^{\nu+1}\Gamma\left(1-\frac{n-\nu}{2}\right)\cdot\Gamma(n+1)} \cdot {}_2F_1\left(\frac{n-\nu}{2}, \frac{n-\nu}{2}; n+1; N_s\right) \quad (14)$$

whilst for $A = B$ both expressions are identical and can be brought into the form:

$$A_{nh} = \frac{\varepsilon_n a_\nu \{\Gamma(\nu+1)\}^2 \sin(n-\nu)\frac{\pi}{2} \cdot A^\nu \left(\frac{n-\nu}{2}\right)}{\pi \cdot 2^{\nu+1}\left\{\Gamma\left(1+\frac{n+\nu}{2}\right)\right\}^2 \Gamma\left(1-\frac{n-\nu}{2}\right)} \quad (15)$$

where $N_s = A^2/B^2$: the signal to "noise" ratio.

* The symbol ${}_2F_1$ denotes the hypergeometric function, which is defined as:

$${}_2F_1(\alpha, \beta; \gamma; x) = \sum_{r=0}^{\infty} \frac{(\alpha)_r (\beta)_r}{r!\,(\gamma)_r} x^r ,$$

where

$$(\alpha)_r = \alpha(\alpha+1)\ldots(\alpha+r-1) = \frac{\Gamma(\alpha+r)}{\Gamma(\alpha)} .$$

From Eqs. (11), (13)—(15) the quotient A_{nh}/A_n is found to be:

$$
\begin{aligned}
N_s > 1: \quad & \frac{A_{nh}}{A_n} = {}_2F_1\left(\frac{n-\nu}{2}, -\frac{n+\nu}{2}; 1; \frac{1}{N_s}\right); \\
N_s = 1: \quad & \frac{A_{nh}}{A_n} = \frac{\Gamma(\nu+1)}{\Gamma\left(1+\frac{n+\nu}{2}\right)\Gamma\left(1-\frac{n-\nu}{2}\right)}; \\
N_s < 1: \quad & \frac{A_{nh}}{A_n} = \frac{N_s^{(n-\nu)/2}\,\Gamma\left(1+\frac{n+\nu}{2}\right)}{\Gamma(1+n)\cdot\Gamma\left(1-\frac{n-\nu}{2}\right)} \\
& \cdot {}_2F_1\left(\frac{n-\nu}{2}, \frac{n-\nu}{2}; n+1; N_s\right).
\end{aligned}
\tag{16}
$$

Fig. 3 shows for different values of n and as a function of the signal to "noise" ratio N_s the calculated A_{nh}/A_n curves for a halfwave linear and a half-wave- quadratic rectifier.

II.3. Correlation Function Method

As mentioned already in I.3, the dynamic characteristics of the linear elements in a system containing a static nonlinearity can be measured directly with the crosscorrelation method of Bussgang (1952). For the nonlinear system of Fig. 4 this method can be demonstrated easily as follows:

The crosscorrelation function $\phi_{xu}(\tau)$ is defined as the expectation of the product of the signals $x(t)$ and $u(t)$:

$$\phi_{xu}(\tau) = E\{x(t)\,u(t+\tau)\}.$$

Using the convolution integral, one finds:

$$\phi_{xu}(\tau) = E\left\{x(t)\int_{-\infty}^{\infty} h_2(v)\,z(t+\tau-v)\,dv\right\},$$

where $h_2(v)$ is the weighting function of the second linear element; $h_2(v)$ and $H_2(j\omega)$ are related by a Fourier transform (see Fig. 4). In a reduced version the theorem of Price (1958) states that for a Gaussian variable y — with zero mean and unity variance — passing through a static nonlinearity $z = f(y)$:

$$E\{x(t)\,z(t+\tau)\} = C\,E\{x(t)\,y(t+\tau)\},$$

where C is a constant determined by the characteristic of the nonlinearity. Substitution of the above expression gives:

$$\phi_{xu}(\tau) = C\int_0^{\infty} h_2(v)\,E\{x(t)\,y(t+\tau-v)\}\,dv.$$

With $x(t)$ a white noise (zero mean value and unity variance) one finds directly:

$$\phi_{xu}(\tau) = C\int_0^{\infty} h_2(v)\,h_1(\tau-v)\,dv.$$

Evidently a sequence of linear processes cannot be split up by this method.

The method of triggered correlation (de Boer and Kuyper, 1968) is related to the above described one. Their method holds for a nonlinearity of a type that takes a sample of one signal $x(t)$ whenever the other signal $y(t)$ passes a pre-set threshold. De Boer and Kuyper (1968) applied their method succesfully to the analysis of spike trains in primary auditory neurons. Although this method has also a linearizing effect, in its present form it is likewise inappropriate to detect a sequence of linear processes.

III. Applications

Three applications of the linearizing method will be presented. The first two deal with the analysis of biological systems and the last one illustrates the synthesis of a physical system.

III.1. Rectification in the Goldfish Retina

A commonly found type of response in the goldfish retina originates from phasic ganglion cells. These ganglion cells are characterized by their response to low frequency stimuli. They give a sustained discharge of spikes during either the positive or negative slope of a low frequency (0.5 cps) triangularly modulated stimulus waveform; to the on or offset of a light stimulus they respond with a short burst of spikes. The descriptive classification of these responses into "on", "off" and "on"-"off" types suggests that the distortion in these ganglion cell responses may be due to rectifying processes, so that phasic units might provide a useful exercise in applying the principles of linearizing.

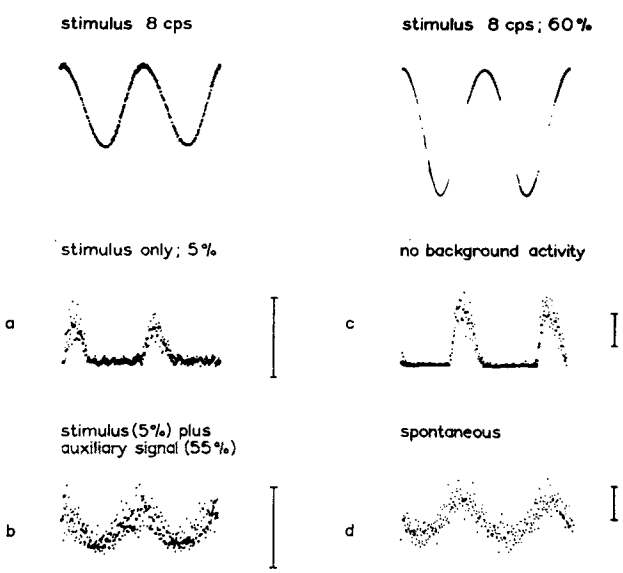

Fig. 7. The responses demonstrate the linearizing effect of an auxiliary signal (first column) and spontaneous spike discharge (second column). The circular light spot focused on the retina has a dia. of 1.2 mm (first column) and 2.5 mm (second column). The number of summations is 300 for Fig. a and 400 for Fig. b—d. The calibration bars are 20 spikes/bin. The bin duration is 625 μsec. In Fig. a and c the lowest points represent the zero count level. This holds approximately also for Fig. b whereas for Fig. d the lowest address points represent a firing rate of the order of 4 spikes/sec. The average intensity of the stimulus passed through a Wratten 29 filter is approximately 1 μW/cm². All responses are from red "off" units

Fig. 7b shows the effect of adding a 0.5 cps triangular auxiliary signal with a modulation depth of 55% to a sinusoidal stimulus of frequency 8 cps and a modulation depth of 5%. In contrast with the half-wave rectified response found when the stimulus is a simple sine wave (Fig. 7a), an almost pure sinusoidal response is found after addition of the triangular auxiliary signal.

An additional interesting feature is the linearizing effect of the neural noise itself. This phenomenon is illustrated in Fig. 7c which shows the usual rectified response from a red "off" unit to a sinusoidal stimulus with a frequency of 8 cps and 60% modulation depth. During the experiment the spontaneous discharge rate was observed to be increasing. When it reached a frequency of 30 spikes per sec an almost linear response was obtained even for a stimulus of 60% modulation depth (Fig. 7d).

These data show that an almost pure sinusoidal response can be obtained either by adding an auxiliary input to the sine wave stimulus or by spontaneously occurring neural noise. Since the amplitude of the fundamental component is not much influenced by the external or internal noise whereas the second harmonic is strongly diminished, the distortions observed in the discharge pattern of the phasic ganglion cells to "small" signal stimulation are of the type produced by a half-wave linear rectifier.

We also studied the dynamic characteristics of the ganglion cell responses and could show that for example a first-order low frequency and third-order high frequency attenuation occurs at a functional stage, preceding the rectifier (Spekreijse, 1969).

III.2. Visually Evoked Scalp Potentials in Man

The visually evoked EEG potentials that can be recorded in man from the scalp electrodes in the occipital region belong to the class of the slow potentials. The responses to sinusoidally modulated light often show considerable harmonic distortion. One of the most striking effects observed for subjects with pronounced α-activity (i.e. the frequency preponderence around 10 cps in the spontaneous EEG) is the appearance of a second harmonic component for a stimulus frequency of about half the α-frequency. In these same subjects the fundamental component dominates in the response when stimulating with a frequency near the α-rhythm. It has been shown that the amplitude of the fundamental component in the response is proportional to the modulation depth of the sinusoidal stimulus, up to a certain value that depends on the size of the visual field, average luminance etc. Such a linear relation holds also for the second harmonic in the response except for a small deviation at modulation depths approaching zero. This deviation can be explained by the influence of quantal noise (van der Tweel and Spekreijse, 1969).

These findings indicate that, just as in the case of the spike discharge in the goldfish retina, the distortions in the human evoked responses can be described — to a first approximation — as linear rectification. This also follows directly from the data given in Fig. 8. This figure shows the linearizing effect of sinusoidal auxiliary inputs. The linearizing effect on the second harmonic decreases as the frequency of the auxiliary input is increased. The amplitude of the fundamental frequency in the response, however, is not effected. This type of experiment leads to the conclusion that high-frequency attenuation occurs before the nonlinear stage in the human visual evoked response system. The transfer function of this attenuating stage has been measured with the method described in I and compares favorable with the data found for the goldfish retina.

III.3. Polarity Coincidence Correlator

The correlation function $\phi_{12}(\tau)$ is a useful tool to detect e.g. hidden periodicity within a signal (autocorrelation) or to provide a quantitative measure of the interdependency between two signals (crosscorrelation). The function is defined as:

$$\phi_{12}(\tau) = \lim_{T\to\infty} \frac{1}{T} \int_0^{+T} x(t)\, y(t+\tau)\, dt \qquad (17)$$

where τ is the independent time-delay variable, T is the integration time, and $x(t)$ and $y(t)$ are the two signals studied.

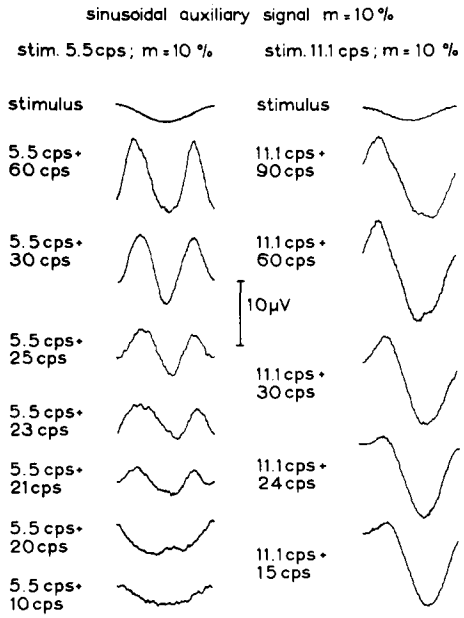

Fig. 8. Occipital responses to sinusoidally modulated light with frequencies of 5.5 cps (left column), and 11.1 cps (right column). Added to this sinusoidal stimulus is a sinusoidal auxiliary signal with the same modulation depth ($A/B = 1$). The left column shows that the effect of decreasing the frequency of this auxiliary signal is to enhance the linearizing effectiveness of the auxiliary signal. This indicates at once that high frequency attenuation preceeds the distorting stage. Since the auxiliary signal has scarcely any influence on the amplitude of the fundamental component in the response (right column), the distortions in the human evoked responses can be ascribed to linear rectification

In most experiments, on-line measurement of $\phi_{12}(\tau)$ is of main importance and sufficient information can be obtained by determining the function at only a discrete set (e.g. 50) of fixed delays τ. These delay units constitute the major difficulty in designing a correlator as it is difficult and expensive to build an accurate delay line with a large number of taps. It is, however, established that only the sign of the signals $x(t)$ and $y(t)$ are sufficient to evaluate $\phi_{12}(\tau)$. Thus this technical problem is greatly simplified, since the delay line consists of a simple shiftregister.

The sign of signals can be determined with a clipper. Since a clipper belongs to the class of rectifiers (0-th order rectifier), the addition of auxiliary signals to the input signal linearizes the output signal. This effect of auxiliary signals on the correlation function has been described for the first time by Veltman and Kwakernaak (1961) and by Jespers et al. (1962).

Following the techniques presented in this paper, Fig. 9 shows for different values of n and as a function of the signal to "noise" ratio N the calculated A_{nh}/A_n curves for an ideal clipper. This figure demonstrates that auxiliary signals can be distinguished by their linearizing effectiveness. A measure for the linearizing effectiveness of an auxiliary signal in the case of an asymmetric nonlinearity is:

$$\text{Lin} = \frac{A_{1h}/A_1}{\sqrt{\sum_{n=2}^{\infty} (A_{nh}/A_n)^2}}, \quad N \ll 1. \tag{18}$$

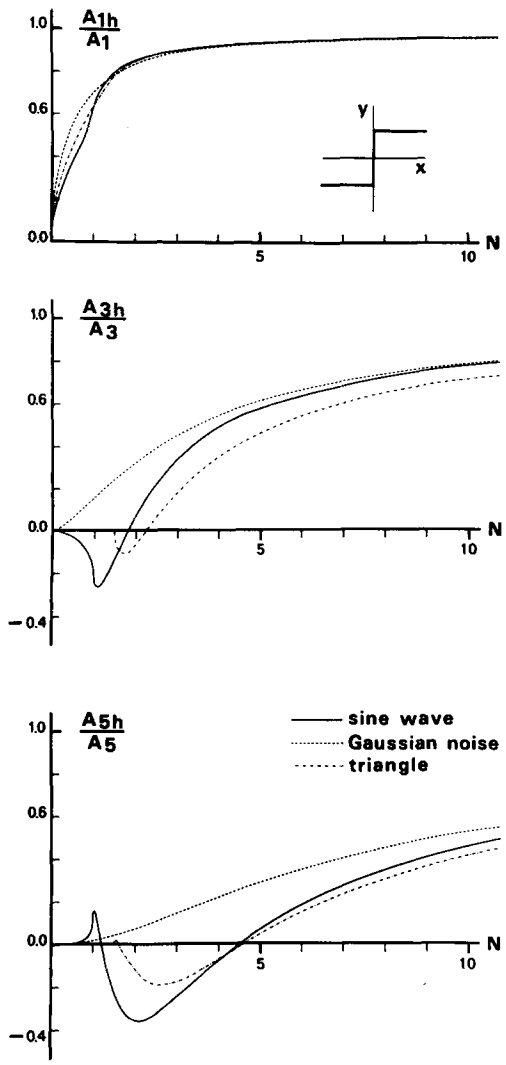

Fig. 9. Linearizing effect of three auxiliary signals — Gaussian noise, triangular and sine wave — upon the amplitudes of the harmonics in the output of an ideal clipper to a sinusoidal input signal. This figure demonstrates that for the given nonlinearity a triangular auxiliary signal is optimal since for signal to noise ratios $N < \frac{3}{2}$ only the fundamental component is present in the output of the clipper

I.e.: that auxiliary signal is optimal, which results in a maximum value of Lin for a given signal to noise ratio N ($N \ll 1$). Based on this criterion, auxiliary signals with rectangular amplitude density distributions have an optimal linearizing effect for an ideal clipper. This follows also directly from Fig. 9, since for $N < 1$ only the fundamental component is present at the output of the clipper, if a triangular auxiliary signal — which has a rectangular amplitude distribution — is used.

These considerations were used in the design of an on-line polarity coincidence correlator that has been built in our laboratory. A shift register, consisting of flip-flops, acts as the delay line. A differently delayed signal is present at each flip-flop, and these can be tapped so as to obtain simultaneously the required number of delays. The autocorrelation function of a sinusoidal signal, measured with this correlator, is presented in Fig. 10 as a function of the amplitudes

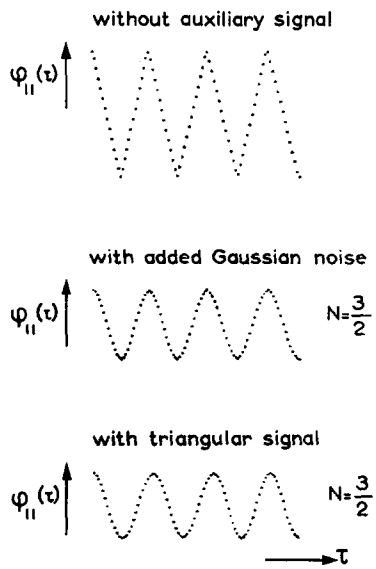

Fig. 10. Autocorrelation functions of a sinusoidal signal measured with a polarity coincidence correlator. The upper curve shows the triangular waveform that is found without auxiliary signal added to the sine wave. The middle curve shows the linearizing effect of a Gaussian noise; the bottom curve is the "real" autocorrelation function, obtained by adding a triangular auxiliary signal to the input sine wave. Comparison of the lower two curves shows that the linearizing effectiveness of a triangular auxiliary signal exceeds that of Gaussian noise

of the two auxiliary signals that are added to both $x(t)$ and $y(t) = x(t+\tau)$. The required statistically independent auxiliary signals with identical rectangular amplitude density distributions can be constructed with a method given by Peek (1967). The curves in Fig. 10 demonstrate that for an auxiliary input of sufficiently large amplitude, a polarity coincidence correlator can be utilized for measuring the real correlation function $\phi_{12}(\tau)$.

Acknowledgements. We are grateful to Dr. Jan Strackee for his help and major advice in this project.

References

Boer, E. de, Kuyper, P.: Triggered correlation. IEEE **BME-15**, 169—179 (1968).

Bussgang, J. J.: Crosscorrelation functions of amplitude distorted Gaussian signals. MIT Res. Lab. Elec. Technical Report **216**, Cambridge, Mass., MIT, March 1952.

Jespers, P., Chu, P. T., Fettweis, A.: A new method for computing correlation functions. Bell Telephone Mfg Co S. A. Antwerpen-Belgium, 1962. For a summary of this paper, see IRE Trans. Information Theory **IT-8**, 106—107 (1962).

Papoulis, A.: The Fourier integral and its applications. New York: McGraw-Hill Book Co., Inc. 1962.

Peek, J. B. H.: The measurement of correlation functions in correlators using "shift-invariant independent" functions. Thesis, Technical Univ. Eindhoven, The Netherlands, (1967).
Price, R. A.: A useful theorem for nonlinear devices having Gaussian inputs. IRE Trans. Information Theory **IT-4**, 69—72 (1958).
Spekreijse, H.: Rectification in the goldfish retina: Analysis by sinusoidal and auxiliary stimulation. Vision Res. **9**, 1461—1472 (1969).
Tweel, L. H. van der, Spekreijse, H.: Signal transport and rectification in the human evoked-response system. Ann. N.Y. Acad. Sci. **156**, 678—695 (1969).
Veltman, B. P. Th., Kwakernaak, H.: Theorie und Technik der Polaritätskorrelation für die dynamische Analyse niederfrequenter Signale und Systeme. Regelungstechnik **9**, 357—364 (1961).
Watson, G. N.: A treatise on the theory of Bessel functions. Cambridge University Press 1962.

Dr. Henk Spekreijse
Laboratory of Medical Physics
University of Amsterdam
Herengracht 196
Amsterdam, Holland

A Mode Control Model of a Neuron's Axon and Dendrites

CHARLES J. SWIGERT*
General Research Corporation, Santa Barbara, California

Received November 25, 1969

Abstract. The ability of a neuron network to process information depends upon the ability of the individual neurons to *transport* impulses and to *control* the signal transport process in other neurons. The transport process for the action potential seen at the axon depends upon the excitable characteristic of the neural membrane. Propagation of signals in the dendrites, where synaptic imputs are most likely processed, is not clearly understood. Extracellular recordings of dendritic systems indicate that the dendrites are partially excitable and can conduct spikes. Further, electrical stimulation of the reticular formation or specific thalamic nuclei suggest that the conduction process can be modified in the dendrites of cortical cells.

A Mode Control model is described which demonstrates many of the observed transport and control properties of dendrite and axon membrane. The model is based upon a simple extension of Fitzhugh's BVP model. Lateral transport over the membrane has been introduced by applying Kirchhoff's laws. Reinterpreting the variables, the influence of membrane potential, pH, and calcium ions can be identified. Modification of the voltage-current characteristic of the membrane model can change the axon model to a dendrite model. The dendrite model possesses a diffusion equation mode, a wave equation mode and a pulse mode. Signals are transferred in the wave and pulse mode and blocked in the diffusion mode. The dendrite's mode is controlled by the "resting" depolarization level. Experimental evidence tends to confirm these phenomena.

I. Introduction

The ability of a neuron network to process information depends upon the ability of the individual neurons both to transport impulses and to control this transport process at other neurons. Following Moruzzi and Magoun's (1949) work on the reticular arousal mechanism, many investigators have observed that the neural signal transfer process can be controlled by neurons in other regions of the brain (Hernandez-Peon, Jung, Towe, Arden and Soderberg). It appears that signal transmission at the nerve is controlled by modification of the temporal response of the nerve. To be more specific, the temporal response of the network depends upon the temporal response of the individual neurons, so that reticular arousal logically implies that the temporal response of the individual neurons can be modified. As an example of the opposite situation, the temporal response of Rall's dendritic membrane model cannot be modified because it is a linear model (Rall). This invariant temporal response of Rall's model implies that the model is uncontrollable. The objective of this paper is to show that:

1. Modification of the neural membrane's temporal response strongly affects signal transmission.

2. Control of the membrane's temporal response can be achieved simply and realistically in a neuron model.

II. Temporal Response of the Neuron and Network

To determine how a neuron network processes an input stimulus, it appears necessary to examine both the spatial and temporal responses of the network. The spatial response of the network, i.e., the spatial transformation carried out upon the imput stimulus by the network, is determined when it is known how each neuron affects each other neuron to which it is connected. The spatial response of the network then describes where an input stimulus can be sent in the network.

The temporal response of the network depends upon the temporal response of the individual neurons (including their synapses) since the neurons transport the signal impulses. It appears to be of fundamental significance that there are reticular mechanisms that can modify the temporal response of the network, which logically implies modification of the temporal response of the individual neurons.

Cortical arousal, electroanesthesia (Tatsuno *et al.*) and the observed variability of evoked responses to identical stimuli (Bremer, Rosenblith) demonstrate the variable temporal response of the neuron network (see Fig. 1). Other researchers have reported ample support for this position: Narikashvilli (1963) has shown that unspecific stimulation in the thalamus or reticular formation markedly facilitates the axon discharges of cortical neurons. Kandel and Tauc (1965) have demonstrated mutual facilitation; a test EPSP[1] being increased 100 to 400 percent. Andersen and Lømo (1966) saw small dendritic spikes invade the soma only if assisted by additional depolarization. Granit

* The work described in this paper was performed while attending the University of California, Berkeley, under a National Institutes of Health Traineeship.

1 EPSP denotes an Excitatory Post Synaptic Potential.